

Increasing the Range of Modulation Indices with the Polarities of Cells and Switching Constraint Reliefs for the Selective Harmonic Elimination Pulse Width Modulation Technique

Mohammad Najjar^{*}, Hossein Iman-Eini[†], and Amirhossein Moeini^{**}

^{*,†}School of Electrical and Computer Engineering, College of Engineering, University of Tehran, Tehran, Iran

^{**}School of Electrical and Computer Engineering, University of Florida, Gainesville, FL, USA

Abstract

In this paper an improved low frequency selective harmonic elimination-PWM (SHE-PWM) technique for Cascaded H-bridge (CHB) converters is proposed. The proposed method is able to eliminate low order harmonics from the output voltage of the converter for a wide range of modulation indices. To solve SHE-PWM equations, especially for low modulation indices, a modified method is used which employs either the positive or negative voltage polarities of H-bridge cells to increase the freedom degrees of each cell. Freedom degrees of the switching angles are also used to increase the range of available solutions for non-linear SHE equations. The proposed SHE methods can successfully eliminate up to 25th harmonic from a 7-level output voltage by using just nine switching transitions or a 150 Hz switching frequency. To confirm the validity of the proposed method, simulation and experimental results have been presented.

Key words: Cascaded H-bridge, Multilevel converter, Particle swarm optimization, Selective harmonic elimination

I. INTRODUCTION

Nowadays, multilevel converters are being widely considered due to their superior performance when compared to conventional inverters. They are categorized into three different structures, cascaded H-bridge, flying capacitor and diode clamped converters. In each structure, the output voltage waveform has a staircase waveform. By increasing the number of voltage levels, it becomes close to a sinusoidal waveform. Some of the features of multilevel converters can be categorized as lower stress across the semiconductors, lower common-mode voltage generation, lower harmonics in the output current and voltage, and lower EMI generation [1], [2]. These converters can be used in high-power applications such as Flexible AC Transmission Systems (FACTS) [3],

High Voltage DC (HVDC) transmission systems [4], and electrical drives [5].

The modulation techniques in multilevel converters are classified according to the switching frequency of the power switches. Employing each of the modulation techniques can provide specific advantages in comparison to the others. For example, the low frequency modulation methods try to eliminate or mitigate low order harmonics from the output voltage or to reduce them to specific levels in order to meet the grid codes, while maintaining a high converter efficiency. Among these methods, selective harmonic elimination-PWM (SHE-PWM) [6]-[21] and [30], selective harmonic mitigation-PWM (SHM-PWM) [22]-[27], and selective harmonic current mitigation PWM [31], [32] have been well established for multilevel converters. The corresponding challenges in these methods are finding the solutions for trigonometric non-linear equations and getting the simplest output waveform pattern while satisfying grid codes from a THD point of view.

In [6], quarter-wave symmetry is used to eliminate the even harmonics from the output voltage of a converter. In this

Manuscript received Nov. 20, 2016; accepted Apr. 8, 2017

Recommended for publication by Associate Editor Liqiang Yuan.

[†]Corresponding Author: imaneini@ut.ac.ir

Tel: +98- 21-61114962, Fax: +98-21-8778690, University of Tehran

^{*}School of Electrical and Computer Engineering, College of Engineering, University of Tehran, Iran

^{**}School of Electrical and Computer Eng, University of Florida, USA

method, the equations of the SHE-PWM are solved in a quarter of period. In [7], half-wave symmetry has been employed. In this method, the number of freedom degrees is increased in comparison to quarter-wave symmetry. However, the number of equations which needs to be solved is almost twice the quarter-wave symmetry, for the same number of switching transitions. In other words, the number of degrees of freedom and the number of solution sets for SHE-PWM are more than those of quarter-wave symmetry. However, extra calculations have to be performed in this method for the same number of switching angles.

In [8], [9], the capacitor voltages in a CHB converter have been considered to be variable in the equations to increase the flexibility of SHE-PWM. In this method, the inverter should be fed by unequal voltages. Hence, it needs variable DC sources for the DC link capacitors according to the values obtained from solving the transcendental equations in SHE-PWM. In addition, SHE-PWM for a Static Synchronous Compensator (STATCOM) based on a CHB has been presented in [10], [11]. In [10], the dc link voltages have different values depending on the amount of losses in each H-bridge. Using constant switching angles and the linear pattern of DC voltage levels to increase the modulation index range has been used in [11].

In the conventional SHE-PWM method, the switching angles of the H-bridge cells should be arranged sequentially after each other. However, in [12], a new method has been presented which tries to omit this criterion. The main feature of this approach is to increase the search space for the optimization method and to have a wider range of available solutions.

To increase the range of available solutions in SHE-PWM, a new method has been proposed in [13], [14] which tries to use either the positive or negative voltage levels of individual cells at switching times. In [14], different switching patterns have been used and various SHE equations based on different patterns are merged into one group of unified SHE equations. Moreover, the inequality constraints on the switching angles are eliminated. In [15], a four-quadrant modulation technique is proposed to extend the modulation index range.

A predictive control formulation for power converters based on SHE-PWM has been proposed in [16]. In this paper the predictive controller modifies the optimal SHE-PWM pattern during transients. A real-time implementation of SHE-PWM is proposed in [17], [18]. To reach this goal, an inner instantaneous observer has been used to extract the harmonic spectrum of the output waveform without applying a FFT algorithm.

The idea of using non-sequential switching angles, when either the positive or negative voltage levels of individual cells have been synthesized to increase the range of available answers in the whole modulation indices is proposed in this paper. By using just nine switching angles in a quarter-cycle

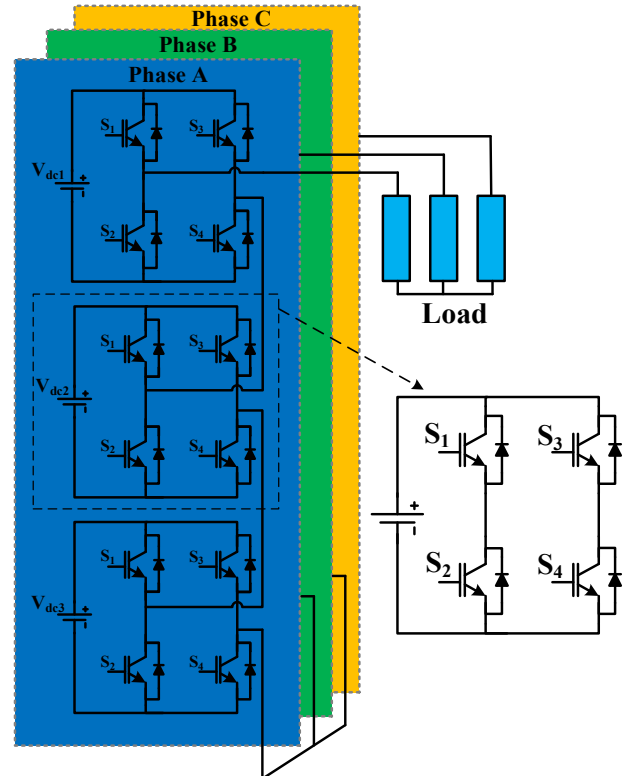


Fig. 1. Structure of a CHB Inverter.

of a fundamental period or a 150 Hz switching frequency, this method can successfully eliminate non-triplen low order harmonics up to the 25th. To verify the validity of the proposed method, simulations and experiments have been carried out on a 7-level CHB inverter.

II. CASCADED H-BRIDGE STRUCTURE

The main multilevel converters are classified as Cascaded H-Bridge (CHB), Neutral Point Clamped (NPC), and Flying Capacitor (FC) [1]. The CHB converter has a lot of advantages among these multilevel converters. It requires a minimum number of components to synthesize the same number of voltage levels and is extremely modular. In addition, the CHB converter has more redundancy states to generate output voltage levels.

Fig. 1 shows a 7-level CHB, which is used in this article. As can be seen, the CHB inverter is made of three series connected H-bridge cells. Each H-bridge cell can generate three different voltage levels, i.e., V_{dc} , 0, and $-V_{dc}$. A larger number of different voltage levels can be obtained by using a series H-bridge.

III. SELECTIVE HARMONIC ELIMINATION (SHE) METHOD

In the SHE-PWM method, a predefined waveform is considered. Then a Fourier series analysis of the predefined

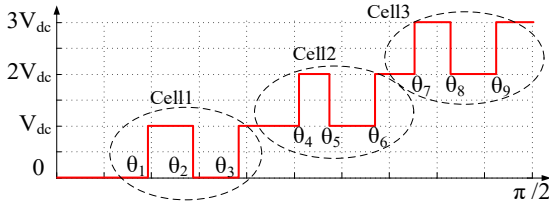


Fig. 2. Predefined waveform for the SHE-PWM technique in a quarter of a period.

output voltage is used to eliminate low order harmonics. Fig. 2 shows a predefined waveform for the SHE-PWM technique in a quarter of a period.

The general equation of SHE-PWM can be expressed as follows:

$$V(\omega t) = \sum_{n=1}^{\infty} (a_n \cos(n\omega t) + b_n \sin(n\omega t)) \quad (1)$$

where ω is the output frequency in radian, and a_n and b_n are the coefficients of the Fourier series. In this formula, the a_n coefficients are omitted from the output harmonic spectra. This is due to the quarter-wave symmetry, which is available in the predefined waveform in Fig. 2.

The b_n coefficients can be written as:

$$b_n = \frac{4V_{dc}}{n\pi} \sum_{i=1}^N r_i \cos n\theta_i \quad n = \text{odd} \quad (2)$$

where V_{dc} is voltage of the DC links, and r is 1 and -1 for the rising and falling edge transitions, respectively.

One of the main purposes of the SHE-PWM method is to control the fundamental value of the output voltage and to eliminate selected harmonics from the output voltage in order to increase the efficiency of the converter.

$$m_a = \sum_{i=1}^N r_i \cos \theta_i \quad (3)$$

where m_a is the amplitude of the fundamental component, and it can vary between 0 and 3 for a 7-level CHB converter.

The output waveform can have a different frequency based on the frequency of the reference. In addition, this method can be used in different multilevel inverters.

IV. PROPOSED SHE-PWM ALGORITHM

A. SHE-PWM Equations

In previous studies [6]-[9], it has been shown that each cell starts to conduct after the last transition of the previous cell. In other words, in each quarter-wave, the switching angles must be generated sequentially and they cannot interfere with each other, as shown for the 7-level waveform in Fig. 2 (cell 1, cell 2 and cell 3). In this figure the first, second and third cells should switch between $(\theta_1-\theta_3)$, $(\theta_4-\theta_6)$, and $(\theta_7-\theta_9)$, respectively. This idea is shown in the following equation for a waveform with three cells, which have three transitions:

$$0 < \overbrace{\theta_1 < \theta_2 < \theta_3}^{\text{Cell 1}} < \overbrace{\theta_4 < \theta_5 < \theta_6}^{\text{Cell 2}} < \overbrace{\theta_7 < \theta_8 < \theta_9}^{\text{Cell 3}} < \frac{\pi}{2} \quad (4)$$

In this paper, to get more freedom degrees to find more

solution sets, another switching limit has been used [10]. This rule is written as:

$$\begin{aligned} \text{cell 1: } 0 < \theta_1 < \theta_2 < \theta_3 < \frac{\pi}{2} \\ \text{cell 2: } 0 < \theta_4 < \theta_5 < \theta_6 < \frac{\pi}{2} \\ \text{cell 3: } 0 < \theta_7 < \theta_8 < \theta_9 < \frac{\pi}{2} \end{aligned} \quad (5)$$

Based on this rule, there is no constraint for the cells to have a regular transition between 0 and $\pi/2$. In other words, the second and other cells can start to conduct even before finishing the transition of the first cell. This feature makes it possible to obtain various predefined waveforms for SHE-PWM algorithms based on a solution set. Moreover, it is easy to apply optimization methods in search of solution sets for non-linear equations.

In order to increase the range of the modulation indices, the idea of positive and negative polarities is also used. In this method, to obtain a wide range of modulation indices, each cell of a CHB converter is allocated to work in both the positive and negative polarities, and even the output half-cycle is positive or negative. Moreover, this modulation strategy can be employed in different multilevel converter structures with any number of voltage levels.

To simplify the switching patterns, the rising edge and falling edge are shown as “↑” and “↓”, respectively. In this paper, each cell has three transitions in a quarter cycle (a 150 Hz switching frequency). Thus, for a positive polarity, the first transition at the H-bridge is the rising edge and all of the transitions in a quarter cycle can be shown as “↑↓↑”. On the other hand, for a negative polarity, the first transition at the H-bridge is the falling edge and all of the transitions in a quarter cycle can be shown as “↓↑↓”.

In this article a 7-level output waveform with nine switching transition is considered (each cell has three transitions). Based on the above considerations, two states can be considered for the CHB switching sequences:

- 1) positive-negative-positive sequence (cell1: ↑↓↑, cell2: ↓↑↓, cell3: ↑↓↑)
- 2) positive-positive-positive sequence (cell1: ↑↓↑, cell2: ↑↓↑, cell3: ↑↓↑)

These states are shown in Fig. 3. By using the second sequence, the polarities of the first, second and third cells are assigned as positive, negative and positive, respectively, in Fig. 3(a). Thus, the output waveform has a lower number of voltage levels. However, it can completely eliminate the low order harmonics from the output voltage. Since the switching constraints of each cell of the CHB converter are independent of the other cell switching constraints in (5), the polarities of the switching can be any of the p-p-n, n-p-p, or p-n-p sequences. On the other hand, in the second case where the polarities of the H-bridge cells are positive, positive and positive, the converter produces a 7-level waveform.

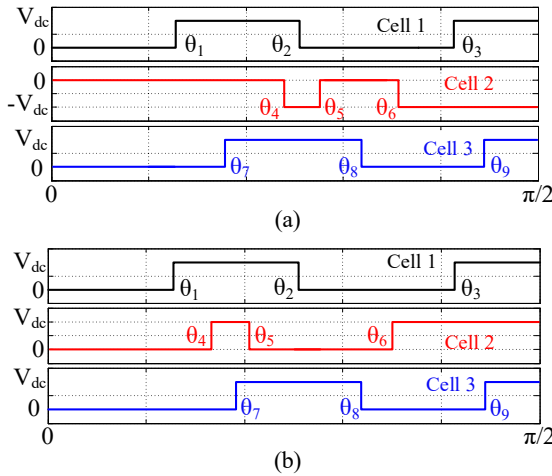


Fig. 3. Switching waveforms of each of the cells in the (a) p-p-n, (b) p-p-p sequence polarities.

The methods used in this paper guarantee the elimination of eight harmonics (i.e. 5th, 7th, 11th, 13th, 17th, 19th, 23th and 25th). In addition, the triplen odd harmonics are eliminated from the output waveform by a three-phase structure.

The equations that are derived from a Fourier analysis are as follows:

For the positive-negative-positive sequence (Fig. 3(a)):

$$\begin{aligned}
 V &= \sum \frac{4V_{dc}}{m\pi} [\cos(m\theta_1) - \cos(m\theta_2) + \cos(m\theta_3) \\
 &\quad - \cos(m\theta_4) + \cos(m\theta_5) - \cos(m\theta_6) + \cos(m\theta_7) \\
 &\quad - \cos(m\theta_8) + \cos(m\theta_9)] \sin m\omega t \\
 \cos(\theta_1) - \cos(\theta_2) + \cos(\theta_3) - \cos(\theta_4) + \cos(\theta_5) \\
 &\quad - \cos(\theta_6) + \cos(\theta_7) - \cos(\theta_8) + \cos(\theta_9) = m_a \\
 \cos(m\theta_1) - \cos(m\theta_2) + \cos(m\theta_3) - \cos(m\theta_4) + \cos(m\theta_5) \\
 &\quad - \cos(m\theta_6) + \cos(m\theta_7) - \cos(m\theta_8) + \cos(m\theta_9) = 0 \\
 m &= 5, 7, 11, 13, 17, 19, 23, 25
 \end{aligned} \quad (6)$$

and for the positive-positive-positive sequence (Fig. 3(b)):

$$\begin{aligned}
 V &= \sum \frac{4V_{dc}}{m\pi} [\cos(m\theta_1) - \cos(m\theta_2) + \cos(m\theta_3) \\
 &\quad + \cos(m\theta_4) - \cos(m\theta_5) + \cos(m\theta_6) + \cos(m\theta_7) \\
 &\quad - \cos(m\theta_8) + \cos(m\theta_9)] \sin m\omega t \\
 \cos(\theta_1) - \cos(\theta_2) + \cos(\theta_3) + \cos(\theta_4) - \cos(\theta_5) \\
 &\quad + \cos(\theta_6) + \cos(\theta_7) - \cos(\theta_8) + \cos(\theta_9) = m_a \\
 \cos(m\theta_1) - \cos(m\theta_2) + \cos(m\theta_3) + \cos(m\theta_4) - \cos(m\theta_5) \\
 &\quad + \cos(m\theta_6) + \cos(m\theta_7) - \cos(m\theta_8) + \cos(m\theta_9) = 0 \\
 m &= 5, 7, 11, 13, 17, 19, 23, 25
 \end{aligned} \quad (7)$$

where m is the harmonic order of the predefined waveform and V_{dc} is the DC link voltage.

B. Solving SHE-PWM Equations

The main problem with harmonic elimination methods is solving non-linear equations. Many different approaches have been proposed to solve these equations [25]-[29]. In this paper, Particle Swarm Optimization (PSO) has been used to

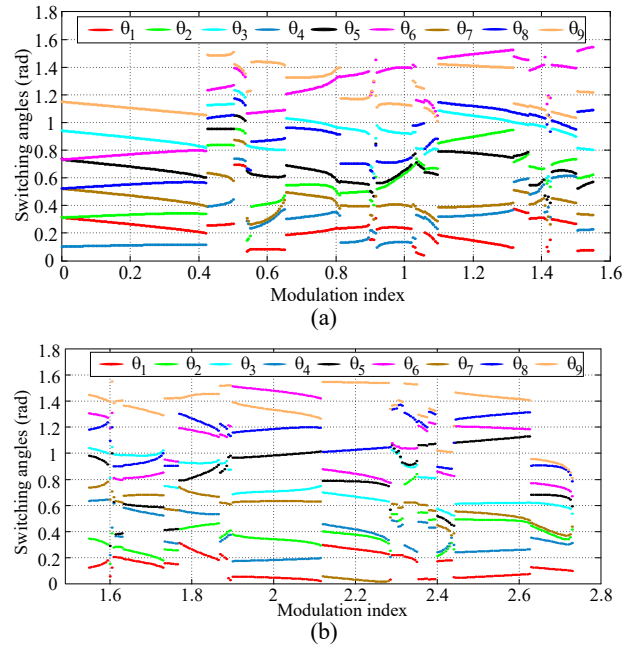


Fig. 4. Obtained answers for the proposed SHE-PWM, when the modulation index interval is: (a) [0, 1.55], (b) [1.55, 2.73].

TABLE I
COMPARISON BETWEEN THE PROPOSED AND CONVENTIONAL TECHNIQUES

Reference	cells	Levels	Angles	Number of eliminated harmonics	The range of Modulation index
[6]	2	5	12	11	0-1.8
[12]	3	7	9	6	0.96-2.73
[14]	4	9	4	3	0-3.45
[21]	3	7	9	8	1.3-2.45
Proposed	3	7	9	8	0-2.73

find switching angles [23]-[25]. The obtained results for two different polarity sequences are shown in Fig. 4. Fig. 4(a) shows the solution when m_a varies between 0 and 1.55. In addition, when it varies between 1.55 and 2.73, the corresponding solutions are shown in Fig. 4(b). Thus, the results are saved as a lookup table and used in practice.

As described earlier, by using the proposed method, different output waveforms have been obtained. The phase voltage (left) and the switching angles in different H-bridge cells (right) for some specific modulation indices are shown in Fig. 5.

C. Comparison

To show the advantages of the proposed technique when compared with conventional techniques, a comparison between them is shown in Table I. As can be seen, [21] uses the same 9 switching angles. However, the modulation range is between 1.3 and 2.5 which is much lower than the obtained range of solution in the proposed technique.

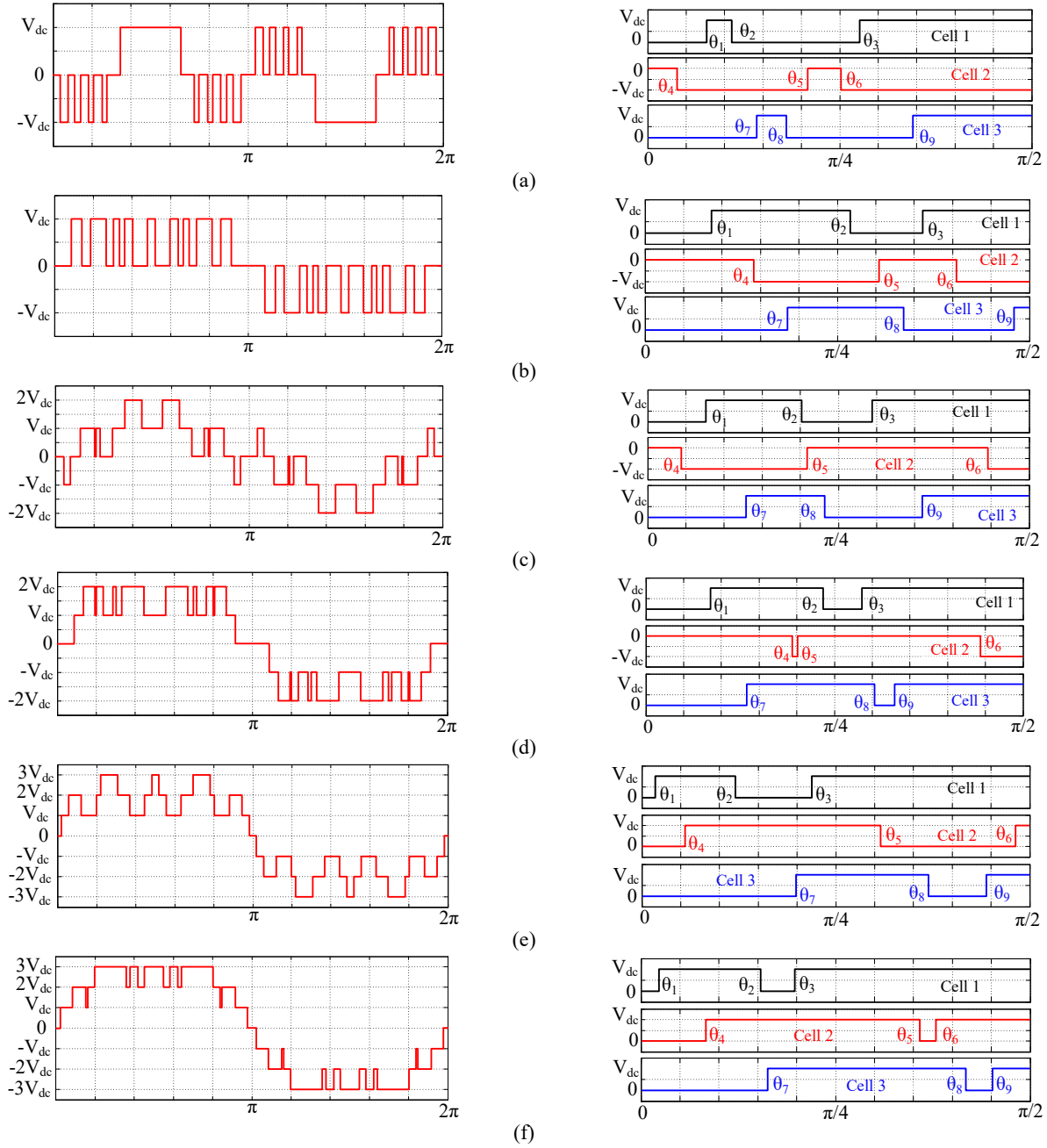


Fig. 5. Output phase voltage (left) and switching angles in different H-bridge cells (right) at different modulation indices: (a) $m_a=0.3$, (b) $m_a=0.5$, (c) $m_a=1$, (d) $m_a=1.5$, (e) $m_a=1.6$, (f) $m_a=2.6$.

TABLE II
SWITCHING ANGLES OF THE PROPOSED METHODS AT DIFFERENT MODULATION INDICES

	$m_a=0.5$	$m_a=0.7$	$m_a=0.9$	$m_a=1.2$	$m_a=1.5$	$m_a=1.8$	$m_a=2.2$	$m_a=2.5$	$m_a=2.7$
θ_1	0.270196 ↑	0.199398 ↑	0.155553 ↑	0.148698 ↑	0.268071 ↑	0.263846 ↑	0.265770 ↑	0.052728 ↑	0.108279 ↑
θ_2	0.838036 ↓	0.551028 ↓	0.440092 ↓	0.899679 ↓	0.738263 ↓	0.436319 ↓	0.377183 ↓	0.492187 ↓	0.352449 ↓
θ_3	1.134718 ↑	1.019938 ↑	0.688811 ↑	1.050825 ↑	0.900491 ↑	0.926805 ↑	0.668601 ↑	0.617895 ↑	0.598155 ↑
θ_4	0.443757 ↓	0.316525 ↓	0.222151 ↓	0.330424 ↓	0.610370 ↓	0.546556 ↑	0.417692 ↓	0.248578 ↓	0.310775 ↓
θ_5	0.955474 ↑	0.673893 ↑	0.5051704 ↑	0.780897 ↑	0.631376 ↑	0.813129 ↓	0.786754 ↓	1.098661 ↑	0.674232 ↓
θ_6	1.271192 ↓	1.228884 ↓	1.198747 ↓	1.49599 ↓	1.393713 ↓	1.178898 ↑	0.844956 ↑	1.204085 ↑	0.742496 ↑
θ_7	0.580797 ↑	0.483135 ↑	0.331824 ↑	0.395911 ↑	0.419154 ↑	0.700491 ↑	0.031502 ↑	0.545843 ↑	0.379883 ↑
θ_8	1.055414 ↓	0.959375 ↓	0.657761 ↓	1.120294 ↓	0.951149 ↓	1.270125 ↓	1.029001 ↓	1.283447 ↓	0.895149 ↓
θ_9	1.510034 ↑	1.327313 ↑	1.208357 ↑	1.410944 ↑	1.035817 ↑	1.447355 ↑	1.546141 ↑	1.447191 ↑	0.918501 ↑

TABLE III
SIMULINK AND EXPERIMENTAL PARAMETERS

Parameter	Symbol	Value
Number of H-Bridge modules	N	3
Nominal DC link voltage of the CHB inverter	V_{DC}	30 V
AC side voltage frequency	f	50 Hz
Switching frequency of inverter	f_{s-i}	150 Hz
Capacitance	C	4 mF
Power MOSFET	S	IRF540N

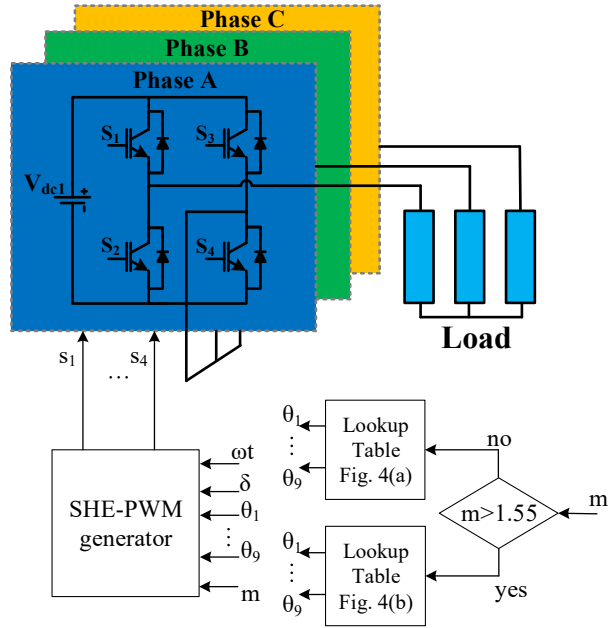


Fig. 6. Block diagram of a 3-phase inverter with the associated SHE-PWM generator.

V. SIMULATION AND EXPERIMENTAL RESULTS

To demonstrate the feasibility of the proposed SHE-PWM method, several simulation and experimental tests have been carried out for different modulation indices. In addition, the MATLAB Simulink environment has been used to simulate a 7-level converter. The switching angles for different modulation indices are shown in Table II. The parameters of the Simulink simulation and hardware prototype are shown in Table. III.

A. Simulation Results

As shown in Table IV, the SHE-PWM can successfully eliminate harmonics up to the 25th harmonic of the output voltage. Furthermore, by using a 3-phase inverter, as shown in Fig. 6, the triplen harmonics are eliminated from the harmonic spectra of the output voltage. In Table IV, the Total Harmonic Distortion (THD) of the voltage waveform is also shown. This parameter shows that the harmonic spectra of the output waveforms are improved when the modulation index of the converter is increased.

A simulation based on Fig. 6 is done to show the phase and line voltage of the inverter when a step change in the

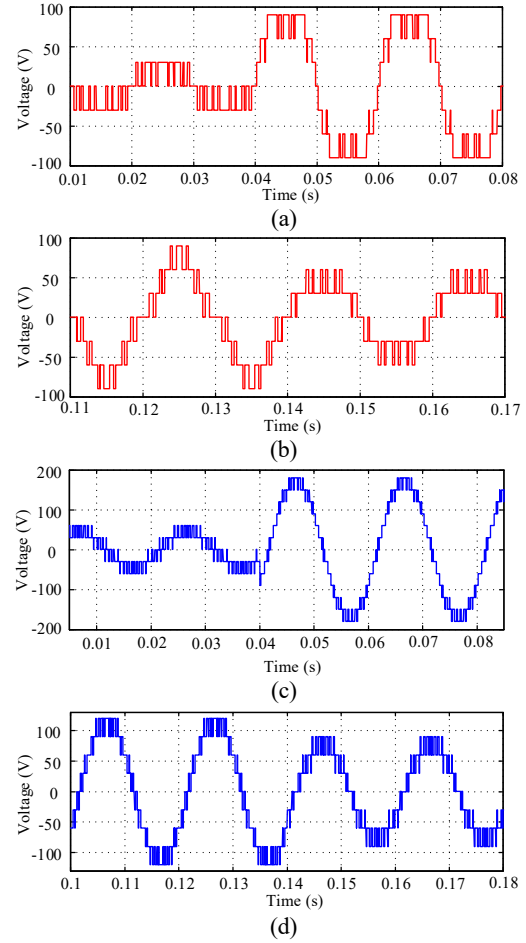


Fig. 7. Simulation results of the AC single-phase line-to-neutral SHM-PWM method for a single-phase converter, when the modulation index is increased from 2 to 2.7: (a) phase voltage when the modulation index is increased from 0.7 to 2.6, (b) phase voltage when the modulation index is decreased from 1.8 to 1.2, (c) line voltage when the modulation index is increased from 0.7 to 2.6, (d) line voltage when the modulation index is decreased from 1.8 to 1.2.

modulation index of the inverter is applied. The phase and line voltages of the output waveforms are shown in Fig. 7.

In Fig. 6, “ ωt ” determines the output frequency of the CHB converter. Thus, different frequencies can be generated depending on the SHE-PWM generator. For example, if the frequency of the reference waveform is 30 Hz, this method eliminates low order harmonics up to the 25th order of harmonic or ($25 \times 30 = 750$ Hz). However, if the reference frequency is 50Hz, then the highest controlled frequency is ($25 \times 50 = 1250$ Hz).

The proposed technique only considers the DC/AC inverter and it uses batteries in the DC side of the inverter to generate AC voltage. In practical applications, another grid-tied converter should be used to provide DC voltage for the DC side of the DC/AC inverter [25],[33], [34].

B. Experimental Results

In this section, the performance of the proposed method is

TABLE IV
VOLTAGE HARMONICS AND THD OF THE PROPOSED SHE-PWM TECHNIQUE, WHEN SIMULATION AND EXPERIMENTAL RESULTS ARE CARRIED OUT AT DIFFERENT MODULATION INDICES

	$m_a=0.5$		$m_a=0.7$		$m_a=0.9$		$m_a=1.2$		$m_a=1.5$		$m_a=1.8$		$m_a=2.2$		$m_a=2.5$		$m_a=2.7$	
	Sim	Exp	Sim	Exp	Sim	Exp	Sim	Exp	Sim	Exp	Sim	Exp	Sim	Exp	Sim	Exp	Sim	Exp
5	0	0.23	0	0.19	0	0.24	0	0.49	0	0.19	0	0.31	0	0.07	0	0.36	0	0.03
7	0	0.66	0	0.59	0	0.39	0	0.57	0	0.21	0	0.17	0	0.04	0	0.31	0	0.10
11	0	0.58	0	0.42	0	0.41	0	0.93	0	0.59	0	0.1	0	0.08	0	0.29	0	0.16
13	0	1.46	0	0.41	0	0.22	0	0.54	0	0.17	0	0.07	0	0.19	0	0.23	0	0.05
17	0	2.34	0	0.39	0	0.24	0	0.95	0	0.28	0	0.18	0	0.24	0	0.07	0	0.19
19	0	1.22	0	0.16	0	0.09	0	0.76	0	0.15	0	0.23	0	0.22	0	0.37	0	0.17
23	0	1.11	0	0.88	0	0.19	0	0.46	0	0.21	0	0.25	0	0.24	0	0.59	0	0.21
25	0	1.12	0	0.96	0	0.62	0	0.49	0	0.16	0	0.35	0	0.42	0	0.30	0	0.17
29	21.92	21.48	27.16	27.0	15.67	15.88	5.79	5.43	10.83	10.68	7.43	7.83	7.39	7.08	3.82	3.76	4.34	4.21
31	19.27	20.4	0.58	1.23	12.75	12.01	16.55	16.23	0.68	0.94	5.26	4.68	2.43	2.84	5.84	5.86	0.48	0.47
35	15.71	14.84	7.21	6.75	12.29	12.88	0.73	0.27	2.13	2.44	3.69	3.73	2.79	2.86	1.82	1.82	1.34	1.54
37	7.76	7.43	12.44	11.31	12.19	11.47	1.73	1.97	0.66	0.62	0.90	0.75	0.95	1.09	0.87	0.87	4.35	4.08
41	0.42	1.59	9.24	9.77	2.84	2.58	1.8	1.66	1.79	1.84	3.15	2.89	0.28	0.41	1.52	1.45	2.42	2.57
43	2.53	2.41	4.03	3.96	0.48	0.53	0.14	0.68	4.19	4.30	2.61	2.62	0.38	0.3	1.34	0.93	1.91	1.69
47	2.15	2.23	4.31	4.25	0.42	0.47	6.11	6.31	4.88	4.77	4.62	4.69	0.57	0.28	2.11	2.46	0.6	0.53
49	2.29	3.13	7.68	7.7	0.81	1.09	6.88	6.32	4.85	4.61	0.76	0.43	1.29	1.41	0.95	1.07	0.02	0.14
THD ^{40th}	34.04	34.13	30.73	30.1	26.60	26.35	17.63	17.33	11.07	11.04	9.86	9.9	8.31	8.24	7.27	7.31	6.30	6.1
THD ^{50th}	34.28	34.47	33.53	33.09	26.77	26.51	19.97	19.58	13.81	13.7	11.66	11.64	8.45	8.38	7.89	7.97	7.04	6.84

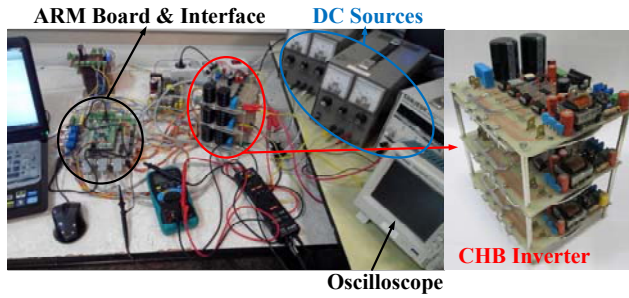


Fig. 8. Hardware prototype of the experimental investigation.

verified by an experimental setup. In practical implementation, a CORTEX M4 ARM processor is used to control the Power MOSFET switches states. The hardware prototype in the experiments is shown in Fig. 8. As can be seen in Table IV, the proposed method can work properly in different modulation indices. In practical implementation, it can be seen that the converter has a higher amount of low order harmonics due to inserting dead times between the power switches and some variations in the voltage of the DC links. However, the amounts of these harmonics are negligible, because they are considerably lower than the existing standards. In addition, the values of the low order harmonics are in good agreement with the simulation results. It is worth noting that the THD, which is shown in the Table IV, is calculated for the harmonics with the Matlab FFT analysis toolbox. Therefore, by using a small filter in the output voltage, the THD of the converter can decrease more.

Waveforms of a practical implementation of the single-phase 7-level CHB converter are shown in Fig. 9, where Fig. 9(a) corresponds to $m_a=0.7$ and Fig. 9(b) corresponds to $m_a=2.7$. The harmonic spectra and THD of the waveforms in Fig. 9, can be found in Table IV. As can be seen, the proposed method can work properly in a wide range of modulation indices without increasing the number of

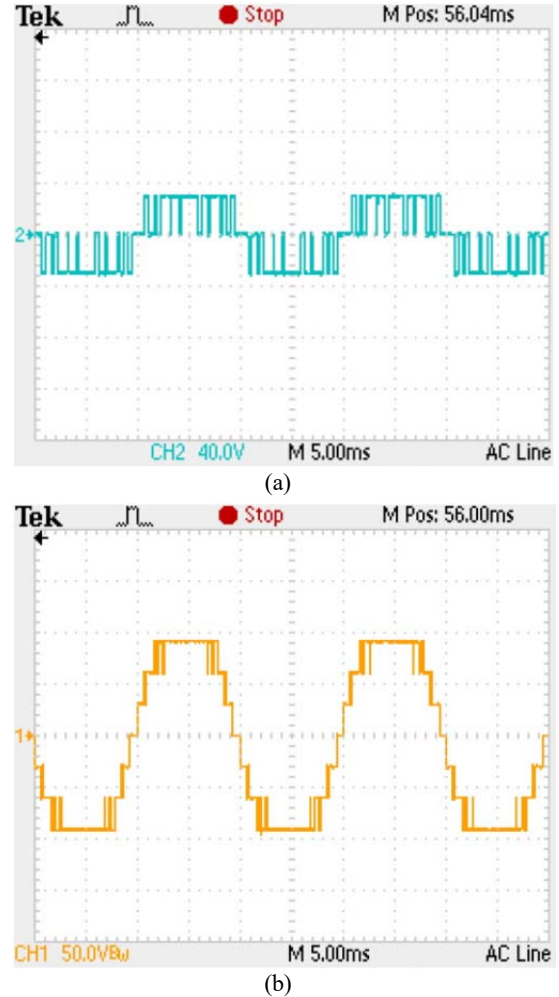


Fig. 9. Practical implementation of the proposed method; (a) $m_a=0.7$, (b) $m_a=2.7$.

switching transitions. Moreover, the harmonic spectra for $m_a=2.7$ is shown in Fig. 10.

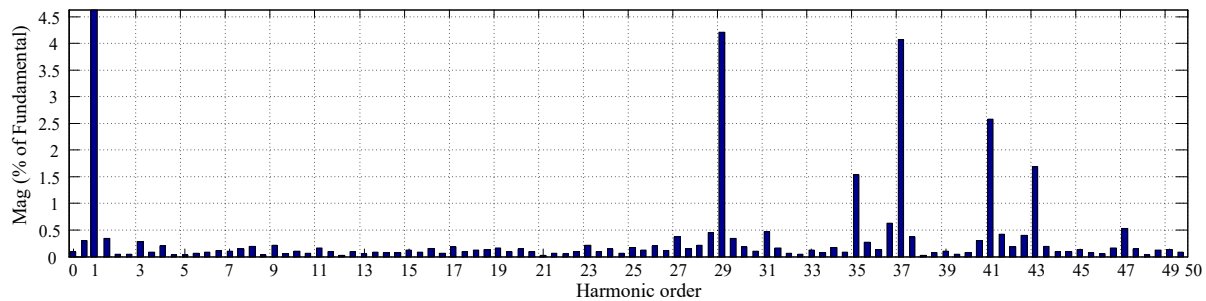


Fig. 10. Harmonic spectra of the experimental results for $m_a=2.7$.

VI. CONCLUSIONS

This paper proposed an improved optimal low frequency SHE-PWM method. The proposed method successfully eliminates the low order harmonics of the converter up to the 25th harmonic. Furthermore, the idea of the opposite polarity cell is used to synthesize a waveform when the modulation index is low. The proposed method can work in a wide range of modulation indices. Therefore, this method can be used in applications that need a wide range of modulation indices.

REFERENCES

- [1] J. Rodriguez, S. Bernet, B. Wu, J. O. Pontt, and S. Kouro, "Multilevel voltage-source-converter topologies for industrial medium-voltage drives," *IEEE Trans. Ind. Electron.*, Vol. 54, No. 6, pp. 2930-2945, Dec. 2007.
- [2] F. Z. Peng, J.-S. Lai, J. W. McKeever, and J. VanCoevering, "A multilevel voltage-source inverter with separate DC sources for static VAr generation," *IEEE Trans. Ind. Appl.*, Vol. 32, No. 5, pp. 1130-1138, Sep./Oct. 1996.
- [3] Q. Song and W. Liu, "Control of a cascade STATCOM with star configuration under unbalanced conditions," *IEEE Trans. Power Electron.*, Vol. 24, No. 1, pp. 45-58, Jan. 2009.
- [4] N. Flourentzou, V. G. Agelidis, and G. D. Demetriades, "VSC-Based HVDC power transmission systems: An overview," *IEEE Trans. Power Electron.*, Vol. 24, No. 3, pp. 592-602, Mar. 2009.
- [5] M. Hagiwara, K. Nishimura, and H. Akagi, "A medium-voltage motor drive with a modular multilevel PWM inverter," *IEEE Trans. Power Electron.*, Vol. 25, No. 7, pp. 1786-1799, Jul. 2010.
- [6] W. Fei, X. Du, and B. Wu, "A generalized formulation of quarter-wave symmetry SHE-PWM problems for multilevel inverters," *IEEE Trans. Power Electron.*, Vol. 24, No. 7, pp. 1758-1766, Jul. 2009.
- [7] W. Fei, X. Du, and B. Wu, "A generalized half-wave symmetry SHE-PWM formulation for multilevel voltage inverters," *IEEE Trans. Ind. Electron.*, Vol. 57, No. 9, pp. 3030-3038, Sep. 2010.
- [8] M. S. A. Dahidah, G. S. Konstantinou, and V. G. Agelidis, "Selective harmonic elimination pulse-width modulation seven-level cascaded H-bridge converter with optimised DC voltage levels," *IET Power Electron.*, Vol. 5, No. 6, pp. 852-862, Jul. 2012.
- [9] L. M. Tolbert, J. N. Chiasson, D. Zhong, and K. J. McKenzie, "Elimination of harmonics in a multilevel converter with nonequal DC sources," *IEEE Trans. Ind. Appl.*, Vol. 41, No. 1, pp. 75-82, Jan.-Feb. 2005.
- [10] M. K. Bakhshizadeh, M. Najjar, F. Blaabjerg, and R. Sajadi, "Using variable DC sources in order to improve the voltage quality of a multilevel STATCOM with low frequency modulation," 2016 18th European Conference on Power Electronics and Applications (EPE'16 ECCE Europe), Karlsruhe, 2016.
- [11] L. K. Haw, M. S. A. Dahidah and H. A. F. Almurib, "SHE-PWM cascaded multilevel inverter with adjustable DC voltage levels control for STATCOM applications," *IEEE Trans. Power Electron.*, Vol. 29, No. 12, pp. 6433-6444, Dec. 2014.
- [12] J. Vassallo, J.C. Clare, P.W. Wheeler, "A power-equalized harmonic-elimination scheme for utility-connected cascaded H-bridge multilevel converters," *The 29th Annual Conference of the IEEE, Industrial Electronics Society*, Vol. 2, pp. 1185-1190, 2003.
- [13] A. Samadi and S. Farhangi, "A novel scheme at low modulation indices for step modulation of h-bridge multilevel converters," *16th Iranian Conference on Electric Engineering*, 2008.
- [14] K. Yang, Q. Zhang, J. Zhang, R. Yuan, Q. Guan, W. Yu, and J. Wang, "Unified selective harmonic elimination for multilevel converters," *IEEE Trans. Power Electron.*, Vol. 32, No. 2, pp. 1579-1590, Feb. 2017.
- [15] H. Zhao and S. Wang, "A four-quadrant modulation technique to extend modulation index range for multilevel selective harmonic elimination/compensation using staircase waveforms," *IEEE J. Emerg. Sel. Topics Power Electron.*, Vol. 5, No. 1, pp. 233-243, Mar. 2017.
- [16] R. Aguilera, P. Acuna, P. Lezana, G. Konstantinou, B. Wu, S. Bernet, and V. Agelidis, "Selective harmonic elimination model predictive control for multilevel power converters," *IEEE Trans. Power Electron.*, Vol. 32, No. 3, pp. 2416-2426, Mar. 2017.
- [17] H. Zhao, T. Jin, S. Wang, and L. Sun, "A real-time selective harmonic elimination based on a transient-free inner closed-loop control for cascaded multilevel inverters," *IEEE Trans. Power Electron.*, Vol. 31, No. 2, pp. 1000-1014, Feb. 2016.
- [18] Y. Liu, H. Hong, and A. Q. Huang, "Real-time calculation of switching angles minimizing THD for multilevel inverters with step modulation," *IEEE Trans. Ind. Electron.*, Vol. 56, No. 2, pp. 285-293, Feb. 2009.
- [19] S. Sirisukprasert, J.-S. Lai, and T.-H. Liu, "Optimum harmonic reduction with a wide range of modulation indexes for multilevel converters," *IEEE Trans. Ind. Electron.*, Vol. 49, No. 4, pp. 875-881, Aug. 2002.
- [20] V. G. Agelidis, A. I. Balouktis, and C. Cossar, "On attaining the multiple solutions of selective harmonic elimination PWM three-level waveforms through function

- minimization," *IEEE Trans. Ind. Electron.*, Vol. 55, No. 3, pp. 996-1004, Mar. 2008.
- [21] A. Moeini, H. Iman-Eini, and A. Marzoughi, "DC link voltage balancing approach for cascaded H-bridge active rectifier based on selective harmonic elimination-pulse width modulation," *IET Power Electron.*, Vol. 8, No. 4, pp. 583-590, Apr. 2015.
- [22] L. G. Franquelo, J. Napoles, R. C. P. Guisado, J. I. Leon, M.A. Aguirre, "A flexible selective harmonic mitigation technique to meet grid codes in three-level PWM converters," *IEEE Trans. Ind. Electron.*, Vol. 54, No. 6, pp. 3022-3029, Dec. 2007.
- [23] A. Moeini, H. Iman-Eini and M. Bakhshizadeh, "Selective harmonic mitigation-pulse-width modulation technique with variable DC-link voltages in single and three-phase cascaded H-bridge inverters," *IET Power Electronics*, Vol. 7, No. 4, pp. 924-932, Apr. 2014.
- [24] A. Marzoughi, H. Iman-Eini, and A. Moeini, "An optimal selective harmonic mitigation technique for high power converters," *International Journal of Electrical Power & Energy Systems*, Vol. 49, pp. 34-39, Jul. 2013.
- [25] M. Najjar, A. Moeini, M. K. Bakhshizadeh, F. Blaabjerg, and S. Farhangi, "Optimal selective harmonic mitigation technique on variable DC link cascaded H-bridge converter to meet power quality standards," *IEEE J. Emerg. Sel. Topics Power Electron.*, Vol. 4, No. 3, pp. 1107-1116, Sep. 2016.
- [26] J. Napoles, A. J. Watson, J. J. Padilla, J. I. Leon, L. G. Franquelo, P. W. Wheeler, and M. A. Aguirre, "Selective harmonic mitigation technique for cascaded h-bridge converters with nonequal DC link voltages," *IEEE Trans. Ind. Electron.*, Vol. 60, No. 5, pp. 1963-1971, May 2013.
- [27] A. Moeini, H. Iman-Eini, and M. Najjar, "Non-equal DC link voltages in a cascaded H-Bridge with a selective harmonic mitigation-PWM technique based on the fundamental switching frequency," *Journal of Power Electronics*, Vol. 17, No. 1, pp. 106-114, Jan. 2017.
- [28] A. Kavousi, B. Vahidi, R. Salehi, M. Bakhshizadeh, N. Farokhnia, and S. S. Fathi, "Application of the bee algorithm for selective harmonic elimination strategy in multilevel inverters," *IEEE Trans. Power Electron.*, Vol. 27, No. 4, pp. 1689-1696, Apr. 2012.
- [29] M. S. A. Dahidah, G. Konstantinou, and V. G. Agelidis, "A review of multilevel selective harmonic elimination PWM: Formulations, solving algorithms, implementation, and applications," *IEEE Trans. Power Electron.*, Vol. 30, No. 8, pp. 4091-4106, Aug. 2015.
- [30] M. Dabbaghjamesh, A. Moeini, M. Ashkaboosi, P. Khazaei, and K. Mirzapalangi, "High performance control of grid connected cascaded H-Bridge active rectifier based on type II-fuzzy logic controller with low frequency modulation technique," *International Journal of Electrical and Computer Engineering*, Vol. 6, No. 2, pp. 484-494, Apr. 2016.
- [31] A. Moeini, H. Zhao, and S. Wang, "A current reference based selective harmonic current mitigation PWM technique to improve the performance of cascaded H-bridge multilevel active rectifiers," *IEEE Trans. Ind. Electron.*, to be published.
- [32] A. Moeini, H. Zhao, and S. Wang, "Improve control to output dynamic response and extend modulation index range with hybrid selective harmonic current mitigation-PWM and phase-shift PWM for four-quadrant cascaded H-bridge converters," *IEEE Trans. Ind. Electron.*, to be published.
- [33] P. Khazaei, S. M. Modares, M. Dabbaghjamesh, M. Almousa, and A. Moeini, "A high efficiency DC/DC boost converter for photovoltaic applications," *International Journal of Soft Computing and Engineering (IJSCE)*, Vol. 6, No. 2, pp. 31-37, May 2016.
- [34] M. Ashkaboosi, S. M. Nourani, P. Khazaei, M. Dabbaghjamesh, and A. Moeini, "An optimization technique based on profit of investment and market clearing in wind power systems," *American Journal of Electrical and Electronic Engineering*, Vol. 4, No. 3, pp. 85-91, 2016.



Mohammad Najjar received his B.S. degree in Electrical Engineering from the Islamic Azad University of Kazeroon, Fars, Iran, in 2010; and his M.S. degree in Power Electronics and Electrical Machines from the University of Tehran, Tehran, Iran, in 2014. His current research interests include multilevel converters, modeling and control of power electronic converters, FACTS devices and power quality issues.



Hossein Iman-Eini (M'10) received his B.S. and M.S. degrees from the University of Tehran, Tehran, Iran, in 2001 and 2003, respectively; and his Ph.D. degree from both the University of Tehran and the Grenoble Institute of Technology, Grenoble, France, in 2009, all in Electrical Engineering. He is presently working as an Associate Professor in the School of Electrical and Computer Engineering, University of Tehran. His current research interests include the modeling and control of power converters, multilevel converters, and renewable energy systems.



Amirhossein Moeini (S'16) received his B.S. degree in Electrical Engineering from the University of Guilan, Rasht, Iran, in 2011; and his M.S. degree in Power Electronics and Electrical Machines from the University of Tehran, Tehran, Iran, in 2013. He is presently working towards his Ph.D. degree in the Power Electronics and Electrical Power Research Laboratory at the University of Florida, Gainesville, FL, USA. His current research interests include modeling and control of power electronic converters, FACTS devices, power quality, evolutionary optimization methods, and optimal modulation techniques.